Proton-Conducting Materials

Deutsche Ausgabe: DOI: 10.1002/ange.201411703
Internationale Ausgabe: DOI: 10.1002/anie.201411703

Superprotonic Conductivity of a UiO-66 Framework Functionalized with Sulfonic Acid Groups by Facile Postsynthetic Oxidation**

*Won Ju Phang, Hyuna Jo, Woo Ram Lee, Jeong Hwa Song, Kicheon Yoo, BongSoo Kim, and Chang Seop Hong**

Abstract: *Facile postsynthetic oxidation of the thiol-laced UiO-66-type framework UiO-66(SH)$_2$ enabled the generation of UiO-66(SO$_3$H)$_2$ with sulfonic acid groups covalently linked to the backbone of the system. The oxidized material exhibited a superprotonic conductivity of 8.4×10^{-2} S cm^{-1} at 80 °C and 90 % relative humidity, and long-term stability of the conductivity was observed. This level of conductivity exceeds that of any proton-conducting MOF reported to date and is equivalent to the conductivity of the most effective known electrolyte, Nafion.*

The increase in the global energy demand caused by rapid industrialization, and concurrent environmental concerns over the massive greenhouse-gas emissions from the combustion of carbon-based fuels, have prompted the pursuit of alternative energy technologies. Among these technologies, fuel cells are electrochemical devices that directly convert chemical energy into electrical energy. The proton-exchange-membrane fuel cell (PEMFC) is recognized to be the most promising system for transportation applications.[1] The redox reaction of hydrogen as a fuel and oxygen as an oxidant in the cell produces water, heat, and electricity; thus, the emission of environmental pollutants is minimized. During the reaction, the oxidized protons at the anode diffuse through the electrolyte membrane to the cathode and encounter electrons from an external circuit. Well-developed PEMFCs comprise perfluorinated polymer membranes (e.g., Nafion) containing terminal sulfonic acid groups that exhibit a proton conductivity as high as 0.10 S cm^{-1} under humid conditions.[2] Alternative materials, such as polysulfones,[3] poly(benzimidazole)s,[4] poly(imide)s, and poly(aryl ether ketone)s[5] have been investigated. However, such aromatic-based polymers require functionalization with sulfonic acid groups for efficient proton conduction.

[*] Dr. W. J. Phang, H. Jo, W. R. Lee, J. H. Song, Prof. C. S. Hong
Department of Chemistry, Korea University
Seoul 136-713 (Korea)
E-mail: cshong@korea.ac.kr
K. Yoo, Dr. B. Kim
Photo-electronic Hybrids Research Center
Korea Institute of Science and Technology (KIST)
Seoul 136-791 (Korea)

[**] This research was supported by a Korea CCS R&D Center (KCRC) grant funded by the Korean government (The Ministry of Science, ICT and Future Planning (MSIP); NRF-2014M1A8A1049253) and the Priority Research Centers Program (NRF20100020209).

Supporting information for this article is available on the WWW under http://dx.doi.org/10.1002/anie.201411703.

Metal–organic frameworks (MOFs) are a class of porous crystalline solids with extremely large surface areas that have been widely explored because of their potential application in various fields, such as gas storage and separation, heterogeneous catalysis, luminescent sensors, and other emerging areas.[6] Noteworthy features include the regularity of the void spaces in the structure, the tunability of the pore size, and the adjustability of the pore surface properties. Such characteristics are beneficial for the development of proton-conducting materials for PEMFC membranes,[1a] since a number of proton-donor and -acceptor sites can be arranged within the conduction pathways of a framework. The conductivity of a material is predominantly determined by the proton mobility and concentration. To increase the number of protons in the framework, the backbone and void space of an MOF can be fine-tuned by two distinct strategies. The first approach involves the encapsulation of guest molecules (e.g., triazole,[7] imidazole,[8] histamine,[9] ammonium cations,[10] or hydronium ions[11]) in the structures. The embedded molecules form a network through hydrogen bonding between the molecules and pre-existent lattice water molecules to construct proton-conduction pathways. The other method involves organic ligands with predesigned acidic moieties, because proton conductivity depends on the pK_a value of the tethered functional groups.[12] As a result of acidic groups covalently bonded to the organic linkers of the backbone, the proton sources are held more securely in the conduction pathway than encapsulated acid molecules, especially under hydrated conditions.

Strong acids (H_2SO_4, H_3PO_4, or trifluoromethanesulfonic acid) readily release protons and supply them to the conduction pathways, thereby permitting high proton conductivity. The acid molecules are usually located in the pore spaces of MOFs for proton conduction.[13] Considering the high performance of Nafion with its terminal sulfonic acid groups, it is desirable to include pendent sulfonic acid groups in the framework for high conductivity. The introduction of noncoordinating sulfonic acid groups into the backbone is prone to be hampered by their tendency to interact with metal ions.[7,14] Postsynthetic modification has been successfully employed to incorporate tuned properties into frameworks for various applications.[15] One interesting study by Goesten et al. showed enhanced acid catalysis and proton conductivity with postsynthetically modified MOFs (MIL-101 and MIL-53) when triflic anhydride and sulfuric acid were used to functionalize the aromatic ring of the linker in the framework.[16] Our strategy takes advantage of the postsynthetic oxidation of a framework to generate sulfonic acid groups tethered to the backbone of the system. This structural

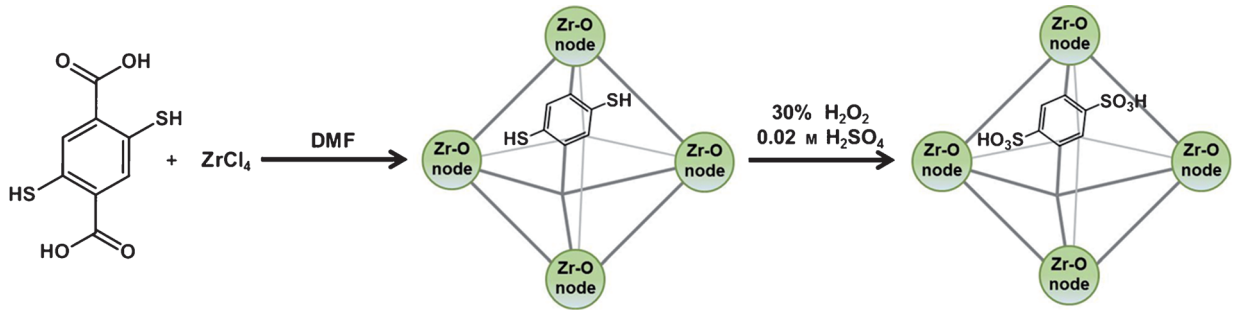

Figure 1. Synthesis of UiO-66(SH)$_2$ and postsynthetic oxidative modification of UiO-66(SH)$_2$ to UiO-66(SO$_3$H)$_2$. DMF = *N*,*N*-dimethylformamide.

feature has not been documented previously for proton-conducting MOFs.

In this study, we used a sturdy UiO-66-type framework with superior water and chemical stability to develop UiO-66(SO$_3$H)$_2$ doubly decorated with sulfonic acid groups with a high density of sulfonic acid groups in the conduction pathways. This material was produced in situ by oxidation of the thiol groups of UiO-66(SH)$_2$. The compound with covalently bound sulfonic acid pendent groups is stable in water under reflux conditions. It reaches a proton conductivity of 8.4×10^{-2} S cm^{-1} (which is much greater than that of pristine UiO-66) at 80 °C and 90 % relative humidity (RH) and maintains good long-term conductivity. The proton conductivity of the material is higher that of current MOF-based proton-conducting materials and is comparable to that of Nafion.

The reaction of Zr^{4+} with 2,5-dimercapto-1,4-benzenedicarboxylic acid (H$_2$DMBDC) in DMF as the solvent and acetic acid as a modulator under microwave irradiation led to the precipitation of the thiol-decorated coordination polymer UiO-66(SH)$_2$ (Figure 1).[17] The UiO-66(SH)$_2$ phase was identified from the powder X-ray diffraction (PXRD) profile, which correlates with the pattern for UiO-66 (Figure 2 a). For

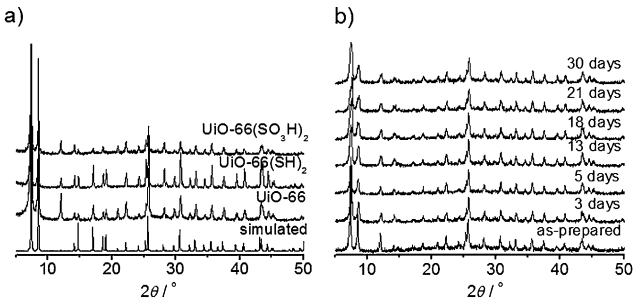

Figure 2. a) PXRD data for UiO-66, UiO-66(SH)$_2$, and UiO-66(SO$_3$H)$_2$, and the simulated spectrum of UiO-66. b) PXRD patterns of UiO-66(SO$_3$H)$_2$ showing its stability in water. The sample was heated at reflux in water for the indicated number of days.

the oxidization of the −SH groups of the framework to −SO$_3$H, this thiol-functionalized material must be stable in H_2O_2 solution. Therefore, we examined the oxidant stability of UiO-66(SH)$_2$ by immersing it in 30 % H_2O_2 solution at room temperature for different time periods. The framework maintained its structural integrity for 48 h (see Figure S1 in the Supporting Information). On the basis of the stability test and other supporting data (see below), we treated UiO-66(SH)$_2$ with H_2O_2 for 1 h, which was the length of time required for full oxidation of the thiol groups. To complete protonation of the sulfonate groups, we suspended the solid in a 0.02 M H_2SO_4 solution for 30 min to form the oxidized product, UiO-66(SO$_3$H)$_2$. The PXRD pattern of UiO-66-(SO$_3$H)$_2$ confirmed that the coordination network remained intact and had the same phase as UiO-66 (Figure 2 a).

The extent of the oxidation of sulfur can be assessed from the X-ray photoelectron spectra (XPS) of UiO-66(SH)$_2$ and UiO-66(SO$_3$H)$_2$ because the binding energy of S $2p_{3/2}$ in −SO$_3$H is blue-shifted with respect to that of S in −SH.[18] The S $2p_{3/2}$ binding energy in UiO-66(SH)$_2$ (163.4 eV) is lower than that in UiO-66(SO$_3$H)$_2$ (167.8 eV), which is indicative of sulfur oxidation (see Figure S2b). To further confirm the presence of −SH and −SO$_3$H functionalities in the samples, we recorded IR spectra of UiO-66, UiO-66(SH)$_2$, and UiO-66(SO$_3$H)$_2$ (see Figure S3). The IR spectrum of UiO-66(SH)$_2$ exhibits a peak at 2570 cm^{-1}, which corresponds to the stretching frequency of free thiol groups and is not visible in the spectrum of UiO-66. In comparison, no thiol peak is visible in the IR spectrum of UiO-66(SO$_3$H)$_2$, and bands centered at 1238 and 1183 cm^{-1} emerge; these bands are assignable to the asymmetric and symmetric stretching frequencies of S=O, respectively. The additional peak at 661 cm^{-1} is attributed to the S−O stretching vibration. The newly observed peaks in the IR spectrum of UiO-66(SO$_3$H)$_2$ clearly suggest the presence of −SO$_3$H groups, as was corroborated by elemental analysis. Thus, the thiol groups in UiO-66(SH)$_2$ are entirely converted into sulfonic acid groups during the H_2O_2 oxidation process and subsequent acid treatment, as also supported by ^{1}H NMR spectroscopy on a digested sample (see Figure S4).

Thermogravimetric (TG) analysis of UiO-66 revealed that an initial weight loss occurs up to 150 °C because of the removal of the attached solvent molecules, and framework decomposition begins at around 500 °C (see Figure S5). A weight loss in UiO-66(SH)$_2$ was evident in the temperature range of 30–320 °C and was attributed to the removal of 1.4 DMF and 22 H_2O lattice molecules, whereas elimination of the lattice water molecules (30 H_2O) in UiO-66(SO$_3$H)$_2$ took place between 30 and 200 °C. The functionalized structures are thermally stable to around 400 °C. MOFs must be robust

towards water for water-mediated proton conduction. We inspected the water stability of UiO-66(SH)$_2$ and UiO-66(SO$_3$H)$_2$ by soaking them in H_2O heated to 100 °C and examining structural variations (Figure 2b; see also Figure S6). From the PXRD profiles, it is evident that the framework structures are retained over 30 days, which demonstrates the significant water stability of the solids. In the scanning electron microscopy (SEM) images, the grain size and morphology of UiO-66 are dissimilar to those of UiO-66(SH)$_2$ and UiO-66(SO$_3$H)$_2$, possibly as a result of the different preparation methods (see Figure S7).

The permanent porosity of the materials was determined by N_2-gas-sorption measurements at 77 K (see Figures S8 and S9). The gas-adsorption experiments involved soaking UiO-66 in methanol for 3 days and then activating it under vacuum at 250 °C for 2 h. UiO-66(SH)$_2$ and UiO-66(SO$_3$H)$_2$ underwent solvent-exchange processes with acetone for 3 days, followed by evacuation at 150 and 120 °C, respectively. The N_2-sorption isotherms at 77 K illustrate type I behavior, which is typical of permanent microporosity. The abrupt rise around 1 bar corresponds to intergrain adsorption. The Brunauer–Emmett–Teller (BET) surface areas are 897 $m^2 g^{-1}$ for UiO-66, 308 $m^2 g^{-1}$ for UiO-66(SH)$_2$, and 35 $m^2 g^{-1}$ for UiO-66(SO$_3$H)$_2$. The order of the surface areas reflects that of the steric bulkiness of the functional groups, which increases from −H to −SH and further to −SO$_3$H, in the pores. The amount of CO_2 adsorbed also increased as the surface area of the pores increased (see Figures S10 and S11).

In a water-mediated system, the framework should favorably adsorb water molecules to generate well-established hydrogen-bonded water networks along the proton-transport pathways. Therefore, we recorded the water-adsorption and -desorption isotherms of UiO-66, UiO-66(SH)$_2$, and UiO-66(SO$_3$H)$_2$ (Figure 3a). The isotherm of UiO-66(SO$_3$H)$_2$ displayed a more rapid increase in the low-pressure region and larger hysteresis than those of the other samples. These features signal that the sulfonic acid groups tethered to the framework have a higher affinity for water than the −H and −SH groups of the other materials. This hydrophilicity should play a key role in enhancing proton transfer. The framework structure is maintained even after water adsorption, as confirmed by the PXRD profiles of the MOFs after adsorption (see Figure S12).

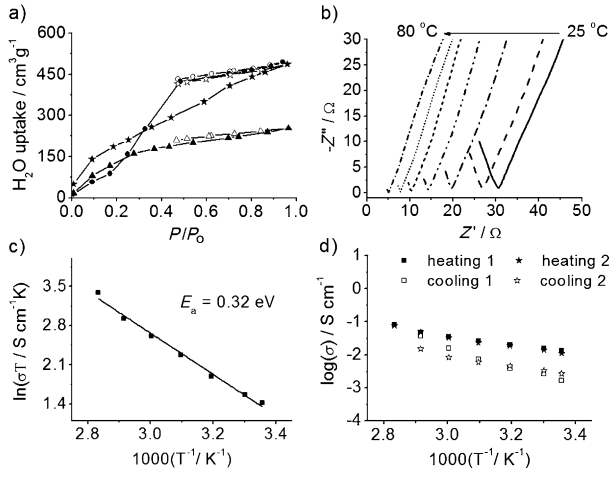

Figure 3. a) Water-vapor-adsorption/desorption isotherms of UiO-66 (circles), UiO-66(SH)$_2$ (triangles), and UiO-66(SO$_3$H)$_2$ (stars) at 25 °C. Filled and open symbols indicate adsorption and desorption, respectively. b) Impedance spectra, c) Arrhenius plot, and d) log-scaled proton conductivities for the heating–cooling cycles of UiO-66(SO$_3$H)$_2$ at 90% RH.

To determine the proton conductivity (σ) of each sample, we measured the alternating-current (ac) impedance spectrum of a pelletized sample from 25 to 80 °C at 90% RH. The conductivities were calculated by fitting the impedance spectra of the samples with a proposed equivalent circuit. Two semicircles are well-resolved in the impedance plots of UiO-66 and UiO-66(SH)$_2$ at different temperatures and 90% RH. These features are probably due to the bulk and intergrain resistance together with the electrode contacts (see Figure S13–S16). The bulk conductivity (3.5×10^{-7} S cm^{-1}) of UiO-66 at 25 °C and 90% RH increased to 4.3×10^{-6} S cm^{-1} at 80 °C and 90% RH. The σ values (6.3×10^{-6} S cm^{-1} at 25 °C and 2.5×10^{-5} S cm^{-1} at 80 °C) of UiO-66(SH)$_2$ under the same conditions are much greater than those of UiO-66. Since the proton-donation ability of a functional group to the hydrogen-bonded water network is governed by the pK_a value,[12] this characteristic originates from the higher acidity of the −SH groups in UiO-66(SH)$_2$ than that of the −H groups in UiO-66. Surprisingly, the conductivity of UiO-66(SO$_3$H)$_2$ increased by more than four orders of magnitude to 1.4×10^{-2} S cm^{-1} at 25 °C and 90% RH when compared to that of UiO-66. At 80 °C, the conductivity was much more pronounced, with a value of 8.4×10^{-2} S cm^{-1} (Figure 3b). Proton transport is possible not only through pores but also through grain boundaries. For example, the water-vapor isotherm of a Cu–TCPP MOF nanofilm (H_2TCPP = 5,10,15,20-tetrakis(4-carboxyphenyl)porphyrin) showed nonporous behavior in the low pressure range and rapid capillary water condensation after $P/P_0 = 0.9$, thus indicating that water adsorption does not occur in the micropore inside the nanosheet but in the mesopores or macropores between the nanosheets.[19] Hence, it is proposed that dominant proton conductivity may arise from the surface of the nanosheet. In contrast, UiO-66(SO$_3$H)$_2$ shows significant water adsorption even at low pressure (Figure 3a), unlike Cu–TCPP, and the initial rise in the isotherm of UiO-66(SO$_3$H)$_2$ was faster than for UiO-66 and UiO-66(SH)$_2$, thus implying enhanced hydrophilic character of UiO-66(SO$_3$H)$_2$. This result suggests that protons in UiO-66(SO$_3$H)$_2$ are primarily conducted through the pores.

This remarkable conductivity (8.4×10^{-2} S cm^{-1}) results from the existence of strong Brønsted acid sites (−SO$_3$H groups) on the organic linkers. These acidic groups facilitate preferential adsorption of water molecules into the confined spaces, which enables organization of the hydrophilic domains and establishes favorable proton-transport pathways, similar to those observed in Nafion. The superprotonic conduction performance (8.4×10^{-2} S cm^{-1}) of UiO-66-(SO$_3$H)$_2$ is superior to that of any proton-conducting MOF materials reported to date.[20] For example, acid-stable solid MIL-101 has been used as a platform to incorporate strong acids into the empty spaces of the framework. The introduc-

tion of H_2SO_4, H_3PO_4, toluenesulfonic acid, and trifluoromethanesulfonic acid (TfOH), into the large nanopores led to conductivities of up to 8×10^{-2} S cm^{-1} (for TfOH@MIL-101) at 60 °C and 15 % RH.[13] Interestingly, both water-mediated ($\sigma=4.2\times10^{-2}$ S cm^{-1} at 98 % RH) and anhydrous proton conductivities ($\sigma=1\times10^{-4}$ S cm^{-1} at 150 °C) were established in a single framework, that is, $\{[(Me_2NH_2)_3(SO_4)]_2[Zn_2(oxalate)_3]\}_n$.[21] These highly proton conducting materials contain guest molecules that facilitate the predominant conduction events, unlike UiO-66$(SO_3H)_2$, which contains strong acid groups that are covalently linked to the organic linkers. This MOF conductor has covalently bound strong acid units that donate high concentrations of protons to the water-mediated conduction channels and facilitate superb conductivity commensurate with that of Nafion.[20,22] The framework stability of all samples was investigated by PXRD after conductivity measurements to deduce the structural robustness of the material (see Figure S17).

The activation energies (E_a) of the materials were derived from Arrhenius plots (Figure 3c; see also Figures S13b and S14b) to be 0.43 eV for UiO-66, 0.23 eV for UiO-66$(SH)_2$, and 0.32 eV for UiO-66$(SO_3H)_2$. These results suggest that functionalization of the interior of the pores creates more-appropriate intervals between the proton-donor and -acceptor sites than those in the nondecorated framework. The determined E_a values of the functionalized solids are similar to those of Nafion (0.22 eV),[23] uranium phosphate (0.32 eV),[24] and many other reported conductive MOFs (see Table S1 in the Supporting Information). The E_a values found for UiO-66$(SH)_2$ and UiO-66$(SO_3H)_2$ lie within the range corresponding to the conventional Grotthuss mechanism, whereby protons supplied by the functional groups diffuse through water channels by a proton-hopping process, which involves fast proton transfer between neighboring $-SO_3^-\cdots H_3O^+\cdots(H_2O)_n$ units and concomitant conformational rearrangement of these entities.

To elucidate the correlation between conductivity and humidity, we measured the proton conductivity for UiO-66$(SO_3H)_2$ at 25 °C with varying relative humidity and plotted the data points on a linear scale (see Figure S18). The conductivity gradually increased in the low RH range and rapidly increased above 50 % RH; this tendency indicates that proton transport relies heavily on the water content in the conduction routes, thus supporting the hypothesis that proton conduction occurs according to the Grotthuss mechanism under water-rich conditions. An analogous feature was also demonstrated in $H^+@Ni_2(dobdc)(H_2O)_2$, for which a steep increase in conductivity was observed when the RH was greater than 75 %.[11]

We carried out temperature-dependent conductivity measurements during two heating and cooling cycles at 90 % RH. The conductivity increased with increasing temperature and decreased during the cooling regime. The discrepancy between the heating and cooling profiles is appreciable and might be related to the degree of sample hydration, because the sample did not have enough time to sufficiently readsorb water molecules during the cooling process. The deviations are more sizable at lower temperatures, possibly as a result of slower kinetics of the adsorption or desorption of water molecules into the conduction pathways.[13a] Because the heating and cooling lines for the two repeated cycles are almost equivalent, the conductivity patterns are predictable, which is a required property for fuel-cell applications. Moreover, the structural integrity was confirmed by the PXRD data of the samples after the heating–cooling cycles (see Figure S19). To test the long-term stability of UiO-66$(SO_3H)_2$, we collected conductivity data after storage of the sample in a controlled humid environment at 90 % RH and 25 °C. The conductivity was nearly invariant up to 96 h, which suggests that the performance is maintained during this time frame. The PXRD pattern of the sample stored in a humid environment for 96 h was consistent with that of the as-prepared sample and indicated that the solid was structurally rigid during the conductivity measurements (see Figure S20). The conductivity of UiO-66$(SO_3H)_2$ after it had been heated at reflux for 30 days was found to be lower than that of a freshly prepared sample under the same measurement conditions owing to local collapse of the framework (see Figure S21). However, its conductivity (2.4×10^{-2} S cm^{-1} at 80 °C and 90 % RH) was still exceptionally high as compared to previously reported values for MOFs (see Table S1).

In summary, we prepared a thiol-laced coordination framework, UiO-66$(SH)_2$, by a microwave-assisted solvothermal reaction. The thiol groups of the solid were fully oxidized with H_2O_2 and treated with H_2SO_4 solution to afford the oxidized product, UiO-66$(SO_3H)_2$. We successfully demonstrated that $-SO_3H$ groups covalently attached to the backbone of an MOF facilitate conductivity by donating labile protons to the conduction channels. The framework structure was maintained even upon heating in water at reflux, which is essential for water-mediated fuel-cell technology. The observed conductivity of 8.4×10^{-2} S cm^{-1} at 80 °C and 90 % RH surpasses that of any MOF-based proton conductors reported to date and is on a par with that of Nafion. In this study, we mimicked the strategy used in Nafion, in which sulfonic acid groups are attached to the terminal groups tethered to the polymeric backbone. The results could provide a promising approach to maximizing the proton-conducting properties of MOF materials.

Keywords: metal–organic frameworks · postsynthetic oxidation · proton-conducting materials · sulfonic acid groups · thiol groups

How to cite: *Angew. Chem. Int. Ed.* **2015**, *54*, 5142 – 5146
Angew. Chem. **2015**, *127*, 5231 – 5235

[1] a) C. Laberty-Robert, K. Vallé, F. Pereira, C. Sanchez, *Chem. Soc. Rev.* **2011**, *40*, 961 – 1005; b) S. J. Peighambardoust, S. Rowshanzamir, M. Amjadi, *Int. J. Hydrogen Energy* **2010**, *35*, 9349 – 9384.
[2] Q. Li, R. He, J. O. Jensen, N. J. Bjerrum, *Chem. Mater.* **2003**, *15*, 4896 – 4915.
[3] J. Kerres, W. Cui, S. Reichle, *J. Polym. Sci. Part A* **1996**, *34*, 2421 – 2438.
[4] E. J. Powers, G. A. Serad, *High Performance Polymers: Their Origin and Development* (Ed.: R. B. Seymour, G. S. Kirshenbaum), Elsevier, New York **1986**, pp. 355 – 373.
[5] D. J. Jones, J. Rozière, *J. Membr. Sci.* **2001**, *185*, 41 – 58.

[6] a) K. Sumida, D. L. Rogow, J. A. Mason, T. M. McDonald, E. D. Bloch, Z. R. Herm, T. H. Bae, J. R. Long, *Chem. Rev.* **2012**, *112*, 724 – 781; b) J. R. Li, J. Sculley, H. C. Zhou, *Chem. Rev.* **2012**, *112*, 869 – 932; c) M. Yoon, R. Srirambalaji, K. Kim, *Chem. Rev.* **2012**, *112*, 1196 – 1231; d) Y. Cui, Y. Yue, G. Qian, B. Chen, *Chem. Rev.* **2012**, *112*, 1126 – 1162; e) P. Falcaro, R. Ricco, C. M. Doherty, K. Liang, A. J. Hill, M. J. Styles, *Chem. Soc. Rev.* **2014**, *43*, 5513 – 5560; f) J. J. Gassensmith, J. Y. Kim, J. M. Holcroft, O. K. Farha, J. F. Stoddart, J. T. Hupp, N. C. Jeong, *J. Am. Chem. Soc.* **2014**, *136*, 8277 – 8282.

[7] J. A. Hurd, R. Vaidhyanathan, V. Thangadurai, C. I. Ratcliffe, I. L. Moudrakovski, G. K. H. Shimizu, *Nat. Chem.* **2009**, *1*, 705 – 710.

[8] S. Bureekaew, S. Horike, M. Higuchi, M. Mizuno, T. Kawamura, D. Tanaka, N. Yanai, S. Kitagawa, *Nat. Mater.* **2009**, *8*, 831 – 836.

[9] D. Umeyama, S. Horike, M. Inukai, Y. Hijikata, S. Kitagawa, *Angew. Chem. Int. Ed.* **2011**, *50*, 11706 – 11709; *Angew. Chem.* **2011**, *123*, 11910 – 11913.

[10] M. Sadakiyo, T. Yamada, K. Honda, H. Matsui, H. Kitagawa, *J. Am. Chem. Soc.* **2014**, *136*, 7701 – 7707.

[11] W. J. Phang, W. R. Lee, K. Yoo, D. W. Ryu, B. Kim, C. S. Hong, *Angew. Chem. Int. Ed.* **2014**, *53*, 8383 – 8387; *Angew. Chem.* **2014**, *126*, 8523 – 8527.

[12] A. Shigematsu, T. Yamada, H. Kitagawa, *J. Am. Chem. Soc.* **2011**, *133*, 2034 – 2036.

[13] a) V. G. Ponomareva, K. A. Kovalenko, A. P. Chupakhin, D. N. Dybtsev, E. S. Shutova, V. P. Fedin, *J. Am. Chem. Soc.* **2012**, *134*, 15640 – 15643; b) D. N. Dybtsev, V. G. Ponomareva, S. B. Aliev, A. P. Chupakhin, M. R. Gallyamov, N. K. Moroz, B. A. Kolesov, K. A. Kovalenko, E. S. Shutova, V. P. Fedin, *ACS Appl. Mater. Interfaces* **2014**, *6*, 5161 – 5167.

[14] a) S. Horike, S. Bureekaew, S. Kitagawa, *Chem. Commun.* **2008**, 471 – 473; b) P. Ramaswamy, R. Matsuda, W. Kosaka, G. Akiyama, H. J. Jeon, S. Kitagawa, *Chem. Commun.* **2014**, *50*, 1144 – 1146.

[15] S. M. Cohen, *Chem. Rev.* **2012**, *112*, 970 – 1000.

[16] M. G. Goesten, J. Juan-Alcañiz, E. V. Ramos-Fernandez, K. B. Sai Sankar Gupta, E. Stavitski, H. van Bekkum, J. Gascon, F. Kapteijn, *J. Catal.* **2011**, *281*, 177 – 187.

[17] K. K. Yee, N. Reimer, J. Liu, S. Y. Cheng, S. M. Yiu, J. Weber, N. Stock, Z. Xu, *J. Am. Chem. Soc.* **2013**, *135*, 7795 – 7798.

[18] Y. Zhou, R. Huang, F. Ding, A. D. Brittain, J. Liu, M. Zhang, M. Xiao, Y. Meng, L. Sun, *ACS Appl. Mater. Interfaces* **2014**, *6*, 7417 – 7425.

[19] G. Xu, K. Otsubo, T. Yamada, S. Sakaida, H. Kitagawa, *J. Am. Chem. Soc.* **2013**, *135*, 7438 – 7441.

[20] P. Ramaswamy, N. E. Wong, G. K. Shimizu, *Chem. Soc. Rev.* **2014**, *43*, 5913 – 5932.

[21] S. S. Nagarkar, S. M. Unni, A. Sharma, S. Kurungot, S. K. Ghosh, *Angew. Chem. Int. Ed.* **2014**, *53*, 2638 – 2642; *Angew. Chem.* **2014**, *126*, 2676 – 2680.

[22] a) S. Horike, D. Umeyama, S. Kitagawa, *Acc. Chem. Res.* **2013**, *46*, 2376 – 2384; b) M. Yoon, K. Suh, S. Natarajan, K. Kim, *Angew. Chem. Int. Ed.* **2013**, *52*, 2688 – 2700; *Angew. Chem.* **2013**, *125*, 2752 – 2764.

[23] a) G. Alberti, M. Casciola, *Solid State Ionics* **2001**, *145*, 3 – 16; b) K. D. Kreuer, S. J. Paddison, E. Spohr, M. Schuster, *Chem. Rev.* **2004**, *104*, 4637 – 4678.

[24] A. T. Howe, M. G. Shilton, *J. Solid State Chem.* **1979**, *28*, 345 – 361.

Received: December 5, 2014
Revised: February 5, 2015
Published online: February 27, 2015

